Published in final edited form as:

Nat Struct Mol Biol. 2008 November ; 15(11): 1160–1168. doi:10.1038/nsmb.1508.

The Janus-Faced Nature of the C_2B Domain Is Fundamental for Synaptotagmin-1 Function

Mingshan Xue[1,*], **Cong Ma**[2,3,*], **Timothy K. Craig**[2,3], **Christian Rosenmund**[1,4,†], and **Josep Rizo**[2,3,†]

[1]Department of Neuroscience, Baylor College of Medicine, One Baylor Plaza, Houston, Texas 77030, USA

[4]Department of Molecular and Human Genetics, Baylor College of Medicine, One Baylor Plaza, Houston, Texas 77030, USA

[2]Department of Biochemistry, University of Texas Southwestern Medical Center, Dallas, 6000 Harry Hines Boulevard, Dallas, Texas 75390, USA

[3]Department of Pharmacology, University of Texas Southwestern Medical Center, Dallas, 6000 Harry Hines Boulevard, Dallas, Texas 75390, USA

Abstract

Synaptotagmin-1 functions as a Ca^{2+} sensor in neurotransmitter release, and was proposed to act on both the synaptic vesicle and plasma membranes through interactions involving the Ca^{2+}-binding top loops of its C_2 domains and the Ca^{2+}-independent bottom face of the C_2B domain. However, the functional importance of the C_2B domain bottom face is unclear. We now show that mutating two conserved arginines at the C_2B domain bottom face practically abolishes synchronous release in hippocampal neurons. Reconstitution experiments reveal that Ca^{2+}/synaptotagmin-1 can dramatically stimulate the rate of SNARE-dependent lipid mixing/fusion and that the two-arginine mutation strongly impairs this activity. These results demonstrate that synaptotagmin-1 function depends critically on the bottom face of the C_2B domain and strongly support the notion that synaptotagmin-1 triggers membrane fusion and neurotransmitter release by bringing the vesicle and plasma membranes together, much like the SNAREs do but in a Ca^{2+}-dependent manner.

The Ca^{2+}-triggered release of neurotransmitters by synaptic vesicle exocytosis is an exquisitely regulated process, exhibiting a fast, synchronous component that emerges in less than 0.5 ms upon Ca^{2+} influx, and a slower, asynchronous component1. Extensive evidence has shown that the synaptic vesicle protein synaptotagmin-1 acts as a Ca^{2+} sensor in synchronous release [reviewed in 1-3]. Most of the cytoplasmic region of synaptotagmin-1 consists of two C_2 domains (called C_2A and C_2B domain), which adopt similar β-sandwich structures and bind three and two Ca^{2+} ions, respectively, through loops at the top of the β-

†To whom correspondence should be addressed. E-mail: rosenmun@bcm.tmc.edu (C.R.); jose@arnie.swmed.edu (J.R.).
*These authors contributed equally to this work.

sandwich4-8 (Fig. 1a). These top loops also mediate Ca^{2+}-dependent binding of both C_2 domains to phospholipids8-11, and decreasing or increasing the apparent Ca^{2+} affinity of synaptotagmin-1 through point mutations in the Ca^{2+}-binding loops leads to parallel changes in the Ca^{2+} dependence of neurotransmitter release12, 13. In addition to establishing the Ca^{2+}-sensing role of synaptotagmin-1 in release, these results showed that the Ca^{2+}-dependent phospholipid binding activity of the C_2 domain top loops is key for this function. Synaptotagmin-1 also binds to the neuronal soluble N-ethylmaleimide-sensitive factor attachment protein receptors (SNAREs), which play a key role in membrane fusion by forming tight SNARE complexes that bring the synaptic vesicle and plasma membranes together [reviewed in1-3, 14, 15]. Ca^{2+}-dependent binding of synaptotagmin-1 to SNARE complexes and phospholipids can occur simultaneously16, 17, which likely helps to couple synaptotagmin-1 and SNARE function.

Many current models assume that synaptotagmin-1 triggers release through an action on the plasma membrane, for instance assisting in membrane fusion by inducing tension1, 3 and/or positive curvature18. However, these models do not explain the observation that disrupting Ca^{2+} binding to the C_2B domain impairs release much more strongly19, 20 than disruption of the C_2A domain Ca^{2+} binding sites21-23. This preponderant role of the C_2B domain in release could arise in part from a polybasic region at one side of the C_2B domain β-sandwich (Fig. 1a) that is not shared by the C_2A domain and has been implicated in multiple interactions, including SNARE complex17, 24 and phospholipid binding25. However, while the moderate impairment in release caused by mutations in this polybasic region supports its involvement in exocytosis25, 26, it does not provide a satisfactory explanation for the dramatic difference in the functional importance of Ca^{2+} binding to the C_2B domain versus the C_2A domain. Another potential reason for this drastic difference was provided by the observation that the C_2B domain can induce clustering of liposomes in the presence of Ca^{2+}, whereas the C_2A domain does not share this activity27. This finding led to a fundamentally different hypothesis of synaptotagmin-1 function proposing that the C_2B domain acts not only on the plasma membrane but also on the vesicle membrane, bringing the two membranes into close proximity like SNARE complexes do, but in a Ca^{2+}-dependent manner that confers the acute Ca^{2+}-sensitivity of synaptic membrane fusion. In this model, the Ca^{2+}-binding loops at the top of the C_2B domain β-sandwich bind to one membrane and basic residues at the opposite, bottom face bind to the other membrane17, 27 (Fig. 1a). However, while the crucial role of the C_2B domain Ca^{2+}-binding region in release is well established19, 20, the functional importance of the bottom face has not been investigated.

We now report that, during electrophysiological studies designed to screen for features at the C-terminus of the C_2B domain that modulate Ca^{2+}-triggered release, we have identified two highly conserved arginines that protrude at the bottom face of the C_2B domain (R398 and R399; Figs. 1a,b) as key residues for synaptotagmin-1 function. Mutation of these arginines almost abolishes Ca^{2+}-triggered fast neurotransmitter release in hippocampal neurons. Further biophysical analyses showed that, in the presence of synaptotagmin-1, Ca^{2+} can induce a dramatic increase in the rate of lipid mixing between reconstituted SNARE proteoliposomes, and that mutating the two arginines strongly impairs this activity due to disruption of C_2B domain-membrane interactions. Our results demonstrate that the Ca^{2+}-independent, bottom face of the synaptotagmin-1 C_2B domain plays a critical function in

neurotransmitter release, similar in importance to the key role of the Ca^{2+}-dependent, top face. Moreover, our data strongly support the notion that synaptotagmin-1 acts on both the vesicle and plasma membranes by bringing them together in a Ca^{2+}-dependent manner through the Janus-faced nature of the C_2B domain.

RESULTS

The two C_2B domain bottom arginines are crucial for release

To test the functional importance of the bottom face of the synaptotagmin-1 C_2B domain, we used a synaptotagmin-1 knockout (KO)-rescue approach in autaptic hippocampal glutamatergic neurons13. In response to a single action potential, the excitatory postsynaptic current (EPSC) amplitude and charge of synaptotagmin-1 KO neurons are drastically reduced, whereas asynchronous release remains unaltered [Ref. 28; Fig. 2]. Lentiviral expression of wild type (WT) synaptotagmin-1 in KO neurons restored the diminished Ca^{2+}-triggered synchronous release to that of WT neurons (Fig. 2 and M.X. and C.R. unpublished results). We next tested the effects of mutating Arg398 and Arg399, the two exposed, highly conserved arginines at the bottom loop between helix HA and strand β8 of the C_2B domain (Fig.1). For this purpose, we prepared single mutants where one arginine was replaced by glutamine (R398Q and R399Q) and a double mutant (R398Q,R399Q), which preserves proper folding of the C_2B domain27 (see also below). Lentiviral expression of these mutants in synaptotagmin-1 KO neurons led to comparable protein levels to those observed for WT synaptotagmin-1 (Supplementary Fig. 1 online), and immunocytochemistry showed that these mutants are co-localized with the synaptic vesicle marker synaptophysin-1, indicating that they are properly targeted to synapses (Supplementary Fig. 2 online). Intriguingly, the R398Q,R399Q mutation practically abolished the rescue activity of synaptotagmin-1. KO neurons rescued by this mutant showed diminished synchronous release, and the evoked EPSC amplitude, charge, and release time course resembled those of synaptotagmin-1 KO neurons (Fig. 2). Both R398Q and R399Q single mutants strongly reduced evoked EPSC amplitude and charge (Figs. 2a-c), but the release remained largely synchronous (Figs. 2a,d). These results demonstrate the critical importance of the bottom region of the C_2B domain for synaptotagmin-1 function in fast neurotransmitter release.

Synaptotagmin-1 has been implicated at multiple steps of the synaptic vesicle cycle. To pinpoint the function of the C_2B domain bottom face, we directly assessed Ca^{2+}-triggered release efficiency by measuring the vesicular release probability (P_{vr}), the fraction of fusion competent vesicles released by an action potential. This parameter is assessed by the ratio of the single EPSC charge and readily releasable vesicle pool (RRP) charge. We measured RRP from the synaptic responses induced by 4–s application of hypertonic sucrose solution29 and found no significant differences in RRP size among all the groups ($P > 0.05$, data not shown). Consequently, mutating either or both arginines caused more than 80% reduction of P_{vr}, as compared to the WT synaptotagmin-1 rescue (Fig. 3a). Consistent with the P_{vr} data, mutating the arginines altered short-term plasticity of rescued KO neurons. In response to 5 consecutive action potentials delivered at 50 Hz, KO neurons rescued by WT synaptotagmin-1 showed synaptic depression, whereas R398Q, R399Q and R398Q,R399Q all led to enhanced synaptic facilitation (Fig. 3b). In contrast to KO neurons, the

R398Q,R399Q-rescued neurons exhibited some synchronous release after 2 or 3 stimuli, indicating that elevation of intracellular Ca^{2+} concentrations can slightly rescue the R398Q,R399Q phenotype (Fig. 3b). We then studied the Ca^{2+}-dependence of transmitter release by measuring the amplitudes of the evoked synaptic responses as a function of the external Ca^{2+} concentrations. Fitting the data with a standard Hill equation revealed a more than 2-fold decrease in the apparent Ca^{2+}-sensitivity of release in KO neurons rescued with single (R398Q or R399Q) or double (R398Q,R399Q) arginine mutants as compared to KO neurons rescued with WT synaptotagmin-1 (Fig. 3c).

The two-arginine mutation impairs membrane interactions

Our electrophysiological results demonstrate that the unique bottom face of the C_2B domain plays an essential role at the Ca^{2+}-triggering step of exocytosis, and support the proposal that binding of the C_2B domain to the vesicle and plasma membranes through the bottom face and the Ca^{2+}-binding top loops is critical for release. However, it is also plausible that the R398Q,R399Q mutation at the bottom of the C_2B domain might have allosteric effects that impair Ca^{2+} binding. This possibility is unlikely because Ca^{2+} binding to the C_2B domain does not change the chemical shifts at the bottom face8 and was completely rule out by comparing ^{1}H-^{15}N HSQC spectra of WT and R398Q,R399Q-C_2AB fragment, which showed that the mutation does not alter Ca^{2+} binding and does not cause substantial structural alterations in the Ca^{2+}-binding loops or any other region of the C_2AB fragment (Supplementary Fig. 3 online). The R398Q,R399Q mutation could also alter synaptotagmin-1/SNARE complex interactions. To test this possibility, we examined the ability of the C_2AB fragment to displace a complexin-1 fragment from SNARE complexes anchored on supported phospholipid bilayers30, an activity that requires Ca^{2+}-dependent phospholipid binding of the top loops of the C_2AB fragment and interactions with SNARE complexes17. The R398Q,R399Q mutation did not substantially change this activity (Fig. 4a), showing that this mutation does not interfere with the C_2AB fragment/SNARE complex interaction.

Based on these results, the most likely explanation for our electrophysiological data is that the inhibition of release by the R398Q,R399Q mutation arises from disruption of critical membrane interactions of the bottom face of the C_2B domain. The R398Q,R399Q mutation abolishes the ability of the synaptotagmin-1 C_2B domain to induce clustering of phospholipid vesicles in vitro27, showing that the bottom face can indeed participate in membrane interactions in vitro. However, the R398Q,R399Q mutation did not appear to impair the ability of the C_2AB fragment to cluster vesicles after a 10 min incubation in 1 mM Ca^{2+} (Ref. 27). To test the effects of this mutation under more stringent conditions, we monitored the ability of different synaptotagmin-1 fragments to induce vesicle clustering as a function of time in the presence of 0.1 mM Ca^{2+} using dynamic light scattering (DLS). The WT C_2AB fragment quickly induced vesicle clustering, as manifested by the observed increase in the average particle size within the first few minutes, and C_2AB fragments with mutations that disrupt Ca^{2+} binding to the C_2A domain ($D178N^{6}$) or the C_2B domain ($D309N^{8}$) exhibited the same clustering activity (Fig. 4b), as observed previously27. Also in agreement with previous results, the isolated C_2B domain clustered vesicles efficiently, and this activity was abolished by the D309N and the R398Q,R399Q mutations (Fig. 4b).

Importantly, the R398Q,R399Q mutation also caused a strong impairment in the ability of the C_2AB fragment to cluster vesicles under these conditions; addition of 1 mM Ca^{2+} after 500 s accelerated clustering by the R398Q,R399Q-C_2AB fragment, leading to large clusters after 10 min, as observed previously27, but the kinetics of clustering was still slower in 1 mM Ca^{2+} than for the WT C_2AB fragment in 0.1 mM Ca^{2+} (Fig. 4b). Hence, the bottom face of the C_2B domain is more critical for vesicle clustering than Ca^{2+} binding to either the C_2A or C_2B domain. However, clustering does require Ca^{2+} binding to at least one C_2 domain, as a double D178N,D309N mutation in the C_2AB fragment completely abolished its clustering activity (Supplementary Fig. 4 online).

Fast stimulation of lipid-mixing by Ca^{2+}/synaptotagmin-1

To further investigate the minimal requirements for the role of the R398Q,R399Q mutation with a defined reductionist system, we turned to reconstitution experiments with SNARE-containing proteoliposomes, in which the ability of protein components to induce lipid mixing is used as an indication of their potential roles in membrane fusion31. Early studies using a standard fluorescence dequenching assay31 showed that the Ca^{2+}-bound synaptotagmin-1 C_2AB fragment can increase the rate of SNARE-dependent lipid mixing32. For our studies, we adopted an approach whereby SNARE complex assembly is facilitated by preincubation of the t-SNARE liposomes with a peptide containing the C-terminal half of the synaptobrevin SNARE motif33. Incubation of equal amounts of t-SNARE and v-SNARE liposomes containing 1:200 protein-to-lipid (P/L) ratios leads to very efficient and saturable lipid mixing (Supplementary Fig. 5a online), as described33. Conversion of the observed fluorescence dequenching to rounds of liposome fusion34 showed that saturation occurs at 1.16 rounds of fusion (Supplementary Fig. 5b online), which suggests that fusion is quantitative under these conditions and corresponds to an increase in relative fluorescence with respect to the initial value (F/F_0) of 1.52. Since in our hands representation of lipid mixing assays using F/F_0, as adopted by Pobbati et al.33, yields more consistent results than conversion to rounds of fusion (likely because of variability in the maximum fluorescence observed upon detergent addition, which is used for this conversion), we used the former method to express the lipid mixing data described below (Fig. 5).

As described previously35, Ca^{2+} plus the C_2AB fragment did not enhance lipid mixing at 1:200 P/L ratio (Fig. 5a). Since the absence of a stimulating effect of Ca^{2+}/synaptotagmin-1 most likely arises because the SNAREs are too active at this P/L ratio, in all subsequent experiments we lowered the P/L ratio to 1:500, which markedly decreased the lipid mixing efficiency of the SNAREs alone (Fig. 5a). Inclusion of 1 μM C_2AB fragment in the initial reaction under these conditions did not substantially alter the lipid-mixing rate but, importantly, addition of 0.1 mM Ca^{2+} after 250 s led to a dramatic increase in lipid mixing (Fig. 5b). This effect was SNARE dependent, as it was inhibited by the soluble region of synaptobrevin and the C_2AB fragment did not induce lipid mixing in the absence of SNAREs (Supplementary Fig. 6 online). The lipid-mixing stimulation required the C_2AB fragment and was specific for Ca^{2+}, since 1 mM Ca^{2+} without C_2AB fragment or 1 mM Mg^{2+} in the presence of C_2AB fragment had no effect (Fig.5b). In multiple experiments (e.g. black traces in Figs. 5b,c,f), lipid mixing was saturated at values of F/F_0 above 1.5, which corresponds to at least one round of fusion and thus suggests that fusion is quantitative (see

above). Although there was some variability in the lipid-mixing rates, dramatic increases in these rates (40- to 130-fold) were consistently observed upon Ca^{2+} addition in the presence of the C_2AB fragment. Conversion to rounds of fusion34 and curve fitting yielded a rate of 0.099 ± 0.035 rounds of fusion per second during the initial burst upon Ca^{2+} addition (corresponding to a time constant τ of ca. 10 s).

The two-arginine mutation impairs lipid-mixing stimulation

We next examined the effects of different mutations on the lipid-mixing enhancement caused by the Ca^{2+}-bound C_2AB fragment (Fig. 5). Quantification of stimulation activities was hindered by variability in the background lipid mixing occurring before Ca^{2+} addition and occasional downward baseline drifts after Ca^{2+} addition that may arise in part from sample precipitation (e.g. Fig. 5h). However, consistent estimates of the relative activities of the different synaptotagmin-1 fragments were obtained by measuring the increase in F/F_0 after 40 seconds of Ca^{2+} addition (after subtracting the background of Ca^{2+}-independent lipid mixing) and normalizing the data to the F/F_0 increase measured for the WT C_2AB fragment with the same proteoliposome preparations (Fig. 6). Remarkably, the R398Q,R399Q mutation in the bottom of the C_2B domain strongly impaired the ability of the C_2AB fragment to stimulate lipid mixing (Fig. 5c, 6), even after adding up to 1 mM Ca^{2+} (Fig. 5d). The single R398Q and R399Q mutations also led to marked impairments of the lipid mixing, although to a lesser extent (Fig. 5c, 6). For comparison, we also tested the effects of mutations that disrupt Ca^{2+} binding to the C_2A or C_2B domain (D178N and D309N, respectively). Both mutations impaired lipid-mixing stimulation, but less strongly than the double R398Q,R399Q mutation (Fig. 5e, 6).

Although the effects of the single arginine mutations on lipid-mixing stimulation correlate qualitatively with their inhibitory effects on neurotransmitter release (Fig 2), the latter were much stronger. Moreover, the stronger impairment of lipid-mixing activity caused by the D178N mutation in the C_2A domain, compared to the D309N mutation in the C_2B domain, contrasts with the preponderant role of the C_2B domain in release19-23. This discrepancy was observed previously35 and may arise because the C_2AB fragment likely binds to two apposed membranes in diverse orientations27. Interestingly, we found that the isolated C_2B domain can partially support the Ca^{2+}-induced lipid-mixing enhancement, whereas the isolated C_2A domain does not share this ability (Fig. 5f, 6). Note that previous data suggesting that the C_2B domain cannot increase SNARE-mediated lipid mixing32 may arise from known difficulties in purifying the C_2B domain36 and, indeed, we did not observe lipid-mixing stimulation when we used C_2B domain purified under less stringent conditions (Fig. 5f). Importantly, the ability of properly purified C_2B domain to support the lipid-mixing enhancement was abrogated by both the R398Q,R399Q mutation and the D309N mutation that disrupts Ca^{2+} binding to the C_2B domain (Fig. 5g, 6). Even the single R398Q and R399Q mutations strongly impaired lipid-mixing stimulation by the C_2B domain (Fig. 5h, 6), showing that both arginines cooperate in this activity, as they do in neurotransmitter release. Thus, our data with the isolated C_2 domains correlate with the preponderant role of the C_2B domain in release and with the strong impairment of release caused by disruption of its Ca^{2+}-binding sites or mutations in Arg398 and Arg399 [Figs. 2,3 and refs. 19, 20].

Discussion

Synaptotagmin-1 function is generally assumed to involve an action of the Ca^{2+}-binding top loops of its C_2 domains on the plasma membrane1, 3, 18. Through electrophysiological screens for additional functional sites on the C2B domain, we have now found that two arginines located at its bottom face are crucial for the function of synaptotagmin-1 in neurotransmitter release. These residues are also key for its ability to bring two membranes together and to stimulate SNARE-mediated lipid-mixing in vitro. These results show that synaptotagmin-1 function depends not only on the Ca^{2+}-binding loops but also on the C_2B domain bottom face, and strongly support the notion that synaptotagmin-1 cooperates with the SNARE complex in triggering fast membrane fusion by binding simultaneously to the vesicle and plasma membranes (Fig. 7).

The almost complete abrogation of fast release caused by the double R398Q,R399Q mutation (Fig. 2) is remarkable. Although the functional effects of many point mutations in synaptotagmin-1 have been studied1-3, only mutations in the C_2B domain Ca^{2+}-binding sites lead to a comparably strong impairment of release as assessed with highly sensitivity electrophysiological recordings in mammalian synapses20. Even single mutations in these arginines result in strong inhibition of release (Fig. 2), suggesting that both arginines cooperate in a critical activity. Mutation of both sites does not completely block synaptotagmin-1 function; intriguingly, the R398,R399 double mutant mimicked the synaptotagmin-1 KO phenotype at slow frequency stimulation, yet this mutant was still weakly active in triggering release, as high frequency stimulation slightly restores synchronous release, presumably due to residual activity of the bottom face of the C_2B domain.

The key role of this bottom face in release is unlikely to involve direct interactions of Arg398 and Arg399 with the SNARE complex, since the R398Q,R399Q mutation did not impair the ability of the C_2AB fragment to displace a complexin-1 fragment from membrane-anchored SNARE complexes (Fig. 4a). This observation agrees well with the notion that the Ca^{2+} binding loops and the bottom face of the C_2B domain bind to two apposed membranes, leaving the polybasic region of C_2B domain available for binding to SNARE complexes (Fig. 7)17. Moreover, NBD fluorescence experiments showed that the C_2B domain bottom face interacts with membranes27, and the profound impairment of vesicle clustering activity caused by the R398Q,R399Q mutation (Fig. 4b) demonstrates that interactions of Arg398 and Arg399 with lipids are crucial for the ability of synaptotagmin-1 to bring two membranes together. These findings, together with our lipid mixing assays, strongly suggest that the impairment of neurotransmitter release caused by the R398Q,R399Q mutation is due to disruption of critical C_2B domain-membrane interactions.

Lipid mixing assays need to be interpreted with caution, since they do not necessarily reflect physiological membrane fusion events2. Thus, the relevance of initial data showing that the Ca^{2+}-bound synaptotagmin-1 C_2AB fragment enhances SNARE-dependent lipid mixing32 was unclear, as the enhancement was modest (2-4 fold), the lipid mixing rates were very slow ($\tau > 30$ min32), and the effects of Ca^{2+}-binding site mutations on lipid-mixing stimulation did not correlate well with their effects on release35, 37. Our data show that, in

the presence of 1 μM C_2AB fragment and under our experimental conditions, 100 μM Ca^{2+} can induce a much more dramatic stimulation of lipid mixing (~ 100-fold) and lead to much faster lipid mixing rates (τ ~ 10 s), which are remarkable considering the limitations of these bulk lipid-mixing assays and the mild conditions of our experiments. These observations strongly support the notion that synaptotagmin-1 plays a direct role in enabling fast Ca^{2+}-triggered membrane fusion during release. During the publication of this work, another study showed that preincubation with the C_2AB fragment allows a strong Ca^{2+}-dependent stimulation of SNARE-dependent lipid mixing, which is further enhanced by a synaptobrevin C-terminal peptide38; while the maximum lipid-mixing rates reported (τ ~ 43 s at 1 mM Ca^{2+} and 20 μM C_2AB fragment) were not as fast as those described here, these data likely reflect the same fundamental property of synaptotagmin-1 that underlies our results and also support its proposed role in Ca^{2+}-triggered fusion.

As observed in earlier reconstitutions35, 37, our experiments with C_2AB fragment do not reproduce the relative importance of the C_2 domain Ca^{2+}-binding sites observed in vivo (Fig. 5e,6). This discrepancy may arise because the C_2AB fragment may support lipid-mixing stimulation by binding to two apposed membranes with diverse relative orientations of the two C_2 domains, some of which may be irrelevant in vivo (note that single Ca^{2+}-binding site mutations do prevent vesicle clustering by the C_2AB fragment; Fig. 4b). Despite this caveat, it seems highly unlikely that the lipid-mixing stimulation caused by Ca^{2+} in the presence of C_2AB fragment arises from completely irrelevant interactions. First, the strong impairment of the C_2AB fragment activity in the lipid-mixing assays caused by the R398Q,R399Q mutation (Fig. 5c) shows that this activity depends on some specific interactions, and clearly correlates with the disruption of release caused by this mutation (Fig. 2,3). Second, the isolated C_2B domain, but not the C_2A domain, can support fast Ca^{2+}-induced lipid mixing (Fig. 5f), in agreement with the preponderant role of the C_2B domain for release19-23. Third, lipid-mixing stimulation is abrogated by both the R398Q,R399Q mutation and the D309N mutation that disrupts Ca^{2+} binding when the C_2B domain is used (Fig. 5g), in correlation with the effects of these mutations in vivo [Fig. 2 and refs. 19, 20)]. These observations suggest that our reconstitutions reproduce at least in part the events that lead to Ca^{2+}-triggered neurotransmitter release in vivo.

It is noteworthy that these results were obtained with soluble synaptotagmin-1 fragments, whereas reconstitutions with full-length synaptotagmin-1 have been more difficult due to undesired ‘cis’ interactions with the v-SNARE membrane35 and a tendency to aggregate38. It is plausible that the proper behavior of full-length synaptotagmin-1 may require additional factors present in vivo, while the essence of the function of its C_2 domains can be captured more easily in these in vitro assays with the soluble C_2AB fragment, likely because their function is mostly associated to interactions with Ca^{2+}, phospholipids and the SNAREs. Note in this context that some synaptotagmin isoforms are localized to vesicles and other to the plasma membrane1, and that the synaptotagmin C_2 domains are connected to their TM regions by long linkers, which may allow similar mechanisms of action for the C_2 domains regardless of the membrane localization.

The finding that the Ca^{2+}-independent bottom face of the C_2B domain is so critical for the Ca^{2+}-dependent function of synaptotagmin-1 may seem paradoxical, but can be easily

explained by the overall cooperativity of the system. For instance, the bottom face of one C_2B domain molecule is insufficient for lipid binding in the absence of Ca^{2+}, but its key role in Ca^{2+}-induced vesicle clustering can be explained because accumulation of multiple C_2B domains on one membrane upon Ca^{2+}-dependent binding through its top loops allows cooperation of their bottom faces in binding to a second, closely apposed membrane27. Similar mechanisms, enhanced by specific interactions with SNARE complexes16, 17, 39, likely underlie the key role of the C_2B domain bottom face for lipid mixing in vitro and neurotransmitter release in vivo. The fact that synaptotagmin-1 can bring two membranes together, like the SNAREs do but in a Ca^{2+}-dependent manner, and that the top and bottom surfaces of the C_2B domain involved in this activity are both critical for neurotransmitter release, strongly support the notion that binding of these surfaces to the apposed vesicle and plasma membranes is fundamental for the action of synaptotagmin-1 in membrane fusion and Ca^{2+}-triggering of release (Fig. 7). These observations suggest an attractive mechanism for the exquisite Ca^{2+}-dependence of release whereby assembly of the C-terminus of the neuronal SNARE complex may not provide sufficient energy to bring the two membrane close enough to induce fusion40, and whereby fusion requires cooperation with the Ca^{2+}-dependent activity of synaptotagmin-1 in binding to the two membranes (note that the Ca^{2+} sensitivity of release may also involve inhibition by synaptotagmin-1 and complexins before Ca^{2+} influx27, 30, 38, 41-44). Moreover, the highly positive electrostatic potential provided by the C_2B domain and the SNARE complex C-terminus may help to induce negative curvature on the membranes to accelerate fusion17, 27, a notion supported by theoretical calculations45.

Conversely, a recent study concluded that synaptotagmin-1 causes fusion by inducing positive membrane curvature through the Ca^{2+} binding loops of both C_2 domains18. However, the experimental basis for this model arises from liposome tubulation assays performed in high concentrations of uranyl acetate, an agent that strongly perturbs membranes46, 47, and the C_2AB fragment induces very little tubulation in the absence of this agent27. Moreover, this model does not provide an explanation for the preponderant role of the C_2B domain and predicts that the C_2 domain Ca^{2+} binding loops are oriented towards the fusion pore while the bottom face of the C_2B domain is facing away from the site of fusion (Supplementary Fig. 7a online), which makes it difficult to envisage how the R398Q,R399Q mutation can lead to strong impairment of neurotransmitter release and membrane fusion. Note however that that this model is not completely incompatible with the model of Fig. 7, since bending of the membranes to initiate membrane fusion requires both negative and positive curvature (Supplementary Fig. 7b online).

Regardless of the validity of these models, our data together with previous studies19, 20 conclusively demonstrate that synaptotagmin-1 function depends critically on both the Ca^{2+}-binding top loops and the Ca^{2+}-independent bottom face of the C_2B domain, and suggest that this Janus-faced nature is crucial for triggering membrane fusion at the high speeds required for synchronous neurotransmitter release. It is noteworthy that distinct functions have also been proposed for the top and bottom faces of the rabphilin C_2B domain48, 49, suggesting that the ability to interact with apposed targets may be a general property of a subset of C_2 domains.

METHODS

Animals and cell culture

Synaptotagmin-1 heterozygous mice were obtained from Dr. Thomas Südhof (University of Texas Southwestern Medical Center, USA)28. Synaptotagmin-1 KO mice were generated by interbreeding the heterozygous mice. All procedures for maintenance and use of these mice were approved by the Institutional Animal Care and Use Committee for Baylor College of Medicine and Affiliates. Astrocytes and hippocampal neurons from postnatal day 0 (P0) mice were cultured as described50. Neurons were plated at a density of 300 cm^{-2} on microisland astrocyte feeder layers for autaptic electrophysiology and immunocytochemistry. For western blot analyses of protein expression, neurons were plated at a density of 10,000 cm^{-2} on confluent astrocyte feeder layers.

Lentivirus constructs and production

A lentiviral vector51 was modified and used, in which a human synapsin-1 promoter and a ubiquitin C promoter drive the expression of mouse synaptotagmin-1 and enhanced green fluorescent protein (EGFP), respectively. Standard recombinant DNA techniques were used to generate all synaptotagmin-1 mutations. Lentiviruses were produced as described51 and infected neurons within 24 hours after plating neurons.

Western blotting and immunocytochemistry

Proteins were extracted from cultured neurons and astrocytes as described50. Expression levels of WT and mutant synaptotagmin-1 variants were examined by standard SDS-PAGE and Western blotting. The presynaptic targeting of WT and mutant synaptotagmin-1 variants were examined by immunocytochemistry and confocal microscopy. Neurons were imaged with an 63x oil objective on a Zeiss 510 laser scanning confocal microscope. Images were acquired as z-stacks and processed using NIH ImageJ to create sum projections from the stacks. The primary antibodies (all from Synaptic Systems) were mouse anti-β-Tubulin III (clone 3B11, 1:4000 for Western blotting), mouse anti-synaptotagmin-1 (clone 41.1, 1:10,000 for Western blotting and 1: 100 for immunocytochemistry) and rabbit anti-synaptophysin-1 (1:1000 for immunocytochemistry).

Electrophysiology of autaptic hippocampal neurons

Whole-cell voltage-clamp recordings were performed on approximately equal numbers of neurons from every group in parallel on the same day *in vitro* (day 8–12 *in vitro*) as described50 with modifications. Briefly, the patch pipette solution contained (in mM) 136 KCl, 17.8 HEPES, 1 EGTA, 0.6 $MgCl_2$, 4 ATP-Mg, 0.3 GTP-Na, 12 phosphocreatine and 50 U ml^{-1} phosphocreatine kinase (300 mOsm, pH 7.4). The standard external solution contained (in mM) 140 NaCl, 2.4 KCl, 10 HEPES, 10 glucose, 2 $CaCl_2$, 4 $MgCl_2$ (300 mOsm, pH 7.4). For the apparent Ca^{2+}-sensitivity of release experiments, the external solution contained 1 mM Mg^{2+} and various Ca^{2+} concentrations as indicated. Each test measurement was preceded and followed by a measurement in standard external solution to control for the rundown of synaptic responses. The amplitudes of EPSCs at each Ca^{2+} concentration were normalized to the amplitudes in standard external solution. All data were

then normalized to the maximal value (the response in 12 mM Ca^{2+}). Data were fitted with a standard Hill equation: $Y=M/(1+K_d/X)^n$); *Y*, response amplitudes; *X*, Ca^{2+} concentrations; *M*, maximum response amplitude; K_d, dissociation constant; *n*, Hill coefficient. All experiments were performed at room temperature (23–24 °C). Data were analyzed offline using AxoGraph X 1.0 (AxoGraph Scientific) and KaleidaGraph (Synergy Software). Statistical significance was tested using Student's t-test, one-way analysis of variance, or two-way analysis of variance.

Protein expression and purification

Full-length or a fragment spanning residues 49-96 of rat synaptobrevin-2, full-length human SNAP-25A (with its four cysteines mutated to serines), a rat syntaxin-1A fragment spanning its SNARE motif and transmembrane region (residues 183-288), a rat complexin-1 V61C mutant fragment (residues 26-83), and WT or mutant rat synaptotagmin-1 fragments (C_2A domain, residues 140-267; C_2B domain, residues 271-421; C_2AB fragment, residues 140-421) were expressed in *E. coli* and purified as described6, 8, 27, 30, 33, 36, 52, except for a sample of the WT C_2B domain that was purified by gel filtration on a Superdex 75 column (GE Health Sciences) in PBS (experiment labeled C_2B* in Fig. 5f) instead of our standard procedure36. The D178N, D309N and R398Q,R399Q mutants of the C_2B domain and C_2AB fragment were described previously27, and expression vectors for the single R398Q and R399Q mutants, as well as the D178N,D309N double mutant, were made using standard recombinant DNA techniques.

Lipid mixing assays

Proteoliposomes containing either synaptobrevin-2 (v-SNARE) or SNAP-25A (with its four cysteines mutated to serines) and syntaxin-1A(183-288) (t-SNARE) were reconstituted as described33 except that the P/L ratio was 1:500 unless otherwise indicated. v-SNARE liposomes contained a 5:2:1:1:1 mixture of phosphatidylcholine, phosphatidylethanolamine (PE), phosphatidylserine, phosphatidylinositol, and cholesterol. t-SNARE liposomes contained the same lipid mixture but replacing 20% PE with 17% PE, 1.5% N-NBD-1,2-dipalmitoyl PE and 1.5% N-(lissamine rhodamine B sulfonyl)-1,2-dipalmitoyl PE) (all lipid ratios expressed in mols). Briefly, dried lipid mixtures were resuspended in 20 mM HEPES pH 7.4, 100 mM KCl, 5 mM DTT, 5% (wt/vol) sodium cholate (13.5 mM total lipid). SNARE proteins solubilized in 20 mM sodium cholate were added in the desired ratio and the mixture was passed through a Fast Desalting PC 3.2/10 column (GE Healthcare) in 20 mM HEPES pH 7.4, 150 mM KCl, 1 mM DTT. Lipid and protein recoveries in the resulting proteoliposomes were practically quantitative, as the central 1 mL fraction collected from the size-exclusion column contained 75%-95% of the starting materials based on the lipid absorption at 574 nm and comparison with standard protein samples of know concentration using Coomassie Blue-stained SDS-PAGE gels (see Supplementary Fig. 8 online for a gel of representative proteoliposomes). For lipid mixing assays, v-SNARE and t-SNARE liposomes [the latter mixed with an equimolar amount of synaptobrevin(49-96)] were separately incubated for 1 hr at 37 °C and then mixed at 37 °C in 20 mM HEPES pH 7.4, 150 mM KCl, 1 mM DTT (0.4 mL final volume; 500 nM final protein concentration). NBD fluorescence emission at 538 nm (excitation 460 nm) was monitored with a PTI

spectrofluorimeter. Synaptotagmin-1 fragments (1 μM final concentration) were added at the beginning of the reaction and divalent cations were added after 250 s.

Miscellaneous procedures

Complexin displacement assays were performed in 25 mM HEPES pH7.4, 100 mM KCl, 0.1 mM EGTA, 0.3mM TCEP, 1 mM Ca^{2+} as described17, 30. Briefly, supported bilayers containing assembled SNARE complexes deposited within single microfluidic channels were incubated with 50 nM BODIPY-FL labeled V61C-complexin 1(26-83) for 15 min, and unbound complexin was washed out. Unlabeled WT or R398Q,R399Q mutant C_2AB fragment at the desired concentration was added and incubated for 10 min, followed by a wash with buffer. BODIPY-FL fluorescence was measured with a Leica (Wetzlar, Germany) confocal microscope (TCS SP2) and quantified with Image J (NIH, MD). Average fluorescence intensities measured under each condition were normalized to a control where the complexin-1 fragment was added to plain supported bilayers17.

Vesicle clustering assays were performed basically as described27 but with modifications. Briefly, 100 nm liposomes prepared by extrusion (DOPS/POPC 30:70) were mixed with the corresponding synaptotagmin-1 fragment in 40 mM Hepes (pH 7.5), 100 mM NaCl (0.05 mg ml^{-1} lipids; 0.5 μM protein), and particle size as a function of time after addition of 100 μM Ca^{2+} was measured by DLS using a Protein Solutions DynaPro instrument.

Supplementary Material

Refer to Web version on PubMed Central for supplementary material.

Acknowledgments

We thank Hui Deng and Hongmei Chen for technical assistance, Richard Atkinson for assistance in confocal microscopy, Carlos Lois (Massachusetts Institute of Technology) and Ralf Nehring (Bayolor College of Medicine) for providing the lentiviral vectors, Thomas Südhof (Stanford University) for providing synaptotagmin-1 heterozygous mice, and Raquel Castillejos (Harvard University) for providing silicon masters for molding microchannels. This work was supported by the Baylor College of Medicine Mental Retardation and Developmental Disabilities Research Center, and by NIH grants NS50655 (to C.R.), NS40944 (to J.R.) and GM65364 (to George M. Whitesides, Harvard University).

References

1. Sudhof TC. The synaptic vesicle cycle. Annu Rev Neurosci. 2004; 27:509–547. [PubMed: 15217342]
2. Rizo J, Chen X, Arac D. Unraveling the mechanisms of synaptotagmin and SNARE function in neurotransmitter release. Trends Cell Biol. 2006; 16:339–350. [PubMed: 16698267]
3. Chapman ER. How Does Synaptotagmin Trigger Neurotransmitter Release? Annu Rev Biochem. 2008
4. Sutton RB, Davletov BA, Berghuis AM, Sudhof TC, Sprang SR. Structure of the first C2 domain of synaptotagmin I: a novel Ca2+/phospholipid-binding fold. Cell. 1995; 80:929–938. [PubMed: 7697723]
5. Shao X, Davletov BA, Sutton RB, Sudhof TC, Rizo J. Bipartite Ca2+-binding motif in C2 domains of synaptotagmin and protein kinase C. Science. 1996; 273:248–251. [PubMed: 8662510]
6. Ubach J, Zhang X, Shao X, Sudhof TC, Rizo J. Ca2+ binding to synaptotagmin: how many Ca2+ ions bind to the tip of a C2-domain? EMBO J. 1998; 17:3921–3930. [PubMed: 9670009]

7. Shao X, Fernandez I, Sudhof TC, Rizo J. Solution structures of the Ca2+-free and Ca2+-bound C2A domain of synaptotagmin I: does Ca2+ induce a conformational change? Biochemistry. 1998; 37:16106–16115. [PubMed: 9819203]
8. Fernandez I, et al. Three-dimensional structure of the synaptotagmin 1 c(2)b-domain. Synaptotagmin 1 as a phospholipid binding machine. Neuron. 2001; 32:1057–1069. [PubMed: 11754837]
9. Chapman ER, Davis AF. Direct interaction of a Ca2+-binding loop of synaptotagmin with lipid bilayers. J Biol Chem. 1998; 273:13995–14001. [PubMed: 9593749]
10. Zhang X, Rizo J, Sudhof TC. Mechanism of phospholipid binding by the C2A-domain of synaptotagmin I. Biochemistry. 1998; 37:12395–12403. [PubMed: 9730811]
11. Herrick DZ, Sterbling S, Rasch KA, Hinderliter A, Cafiso DS. Position of synaptotagmin I at the membrane interface: cooperative interactions of tandem C2 domains. Biochemistry. 2006; 45:9668–9674. [PubMed: 16893168]
12. Fernandez-Chacon R, et al. Synaptotagmin I functions as a calcium regulator of release probability. Nature. 2001; 410:41–49. [PubMed: 11242035]
13. Rhee JS, et al. Augmenting neurotransmitter release by enhancing the apparent Ca2+ affinity of synaptotagmin 1. Proc Natl Acad Sci U S A. 2005; 102:18664–18669. [PubMed: 16352718]
14. Brunger AT. Structure and function of SNARE and SNARE-interacting proteins. Q Rev Biophys. 2005:1–47. [PubMed: 16336742]
15. Jahn R, Scheller RH. SNAREs--engines for membrane fusion. Nat Rev Mol Cell Biol. 2006; 7:631–643. [PubMed: 16912714]
16. Bhalla A, Chicka MC, Tucker WC, Chapman ER. Ca(2+)-synaptotagmin directly regulates t-SNARE function during reconstituted membrane fusion. Nat Struct Mol Biol. 2006; 13:323–330. [PubMed: 16565726]
17. Dai H, Shen N, Arac D, Rizo J. A Quaternary SNARE-Synaptotagmin-Ca(2+)-Phospholipid Complex in Neurotransmitter Release. J Mol Biol. 2007; 367:848–863. [PubMed: 17320903]
18. Martens S, Kozlov MM, McMahon HT. How synaptotagmin promotes membrane fusion. Science. 2007; 316:1205–1208. [PubMed: 17478680]
19. Mackler JM, Drummond JA, Loewen CA, Robinson IM, Reist NE. The C(2)B Ca(2+)-binding motif of synaptotagmin is required for synaptic transmission in vivo. Nature. 2002; 418:340–344. [PubMed: 12110842]
20. Nishiki T, Augustine GJ. Dual roles of the C2B domain of synaptotagmin I in synchronizing Ca2+-dependent neurotransmitter release. J Neurosci. 2004; 24:8542–8550. [PubMed: 15456828]
21. Robinson IM, Ranjan R, Schwarz TL. Synaptotagmins I and IV promote transmitter release independently of Ca(2+) binding in the C(2)A domain. Nature. 2002; 418:336–340. [PubMed: 12110845]
22. Fernandez-Chacon R. Structure/function analysis of Ca2+ binding to the C2A domain of synaptotagmin 1. J Neurosci. 2002; 22:8438–8446. [PubMed: 12351718]
23. Stevens CF, Sullivan JM. The synaptotagmin C2A domain is part of the calcium sensor controlling fast synaptic transmission. Neuron. 2003; 39:299–308. [PubMed: 12873386]
24. Rickman C, et al. Conserved prefusion protein assembly in regulated exocytosis. Mol Biol Cell. 2006; 17:283–294. [PubMed: 16267273]
25. Li L, et al. Phosphatidylinositol phosphates as co-activators of Ca2+ binding to C2 domains of synaptotagmin 1. J Biol Chem. 2006; 281:15845–15852. [PubMed: 16595652]
26. Mackler JM, Reist NE. Mutations in the second C2 domain of synaptotagmin disrupt synaptic transmission at Drosophila neuromuscular junctions. J Comp Neurol. 2001; 436:4–16. [PubMed: 11413542]
27. Arac D, et al. Close membrane-membrane proximity induced by Ca(2+)-dependent multivalent binding of synaptotagmin-1 to phospholipids. Nat Struct Mol Biol. 2006; 13:209–217. [PubMed: 16491093]
28. Geppert M, et al. Synaptotagmin I: a major Ca2+ sensor for transmitter release at a central synapse. Cell. 1994; 79:717–727. [PubMed: 7954835]

29. Rosenmund C, Stevens CF. Definition of the readily releasable pool of vesicles at hippocampal synapses. Neuron. 1996; 16:1197–1207. [PubMed: 8663996]
30. Tang J, et al. A complexin/synaptotagmin 1 switch controls fast synaptic vesicle exocytosis. Cell. 2006; 126:1175–1187. [PubMed: 16990140]
31. Weber T, et al. SNAREpins: minimal machinery for membrane fusion. Cell. 1998; 92:759–772. [PubMed: 9529252]
32. Tucker WC, Weber T, Chapman ER. Reconstitution of Ca2+-regulated membrane fusion by synaptotagmin and SNAREs. Science. 2004; 304:435–438. [PubMed: 15044754]
33. Pobbati AV, Stein A, Fasshauer D. N- to C-terminal SNARE complex assembly promotes rapid membrane fusion. Science. 2006; 313:673–676. [PubMed: 16888141]
34. Parlati F, et al. Rapid and efficient fusion of phospholipid vesicles by the alpha-helical core of a SNARE complex in the absence of an N-terminal regulatory domain. Proc Natl Acad Sci U S A. 1999; 96:12565–12570. [PubMed: 10535962]
35. Stein A, Radhakrishnan A, Riedel D, Fasshauer D, Jahn R. Synaptotagmin activates membrane fusion through a Ca(2+)-dependent trans interaction with phospholipids. Nat Struct Mol Biol. 2007; 14:904–911. [PubMed: 17891149]
36. Ubach J, et al. The C2B domain of synaptotagmin I is a Ca2+-binding module. Biochemistry. 2001; 40:5854–5860. [PubMed: 11352720]
37. Bhalla A, Tucker WC, Chapman ER. Synaptotagmin isoforms couple distinct ranges of Ca2+, Ba2+, and Sr2+ concentration to SNARE-mediated membrane fusion. Mol Biol Cell. 2005; 16:4755–4764. [PubMed: 16093350]
38. Chicka MC, Hui E, Liu H, Chapman ER. Synaptotagmin arrests the SNARE complex before triggering fast, efficient membrane fusion in response to Ca2+ Nat Struct Mol Biol. 2008; 15:827–835. [PubMed: 18622390]
39. Bowen ME, Weninger K, Ernst J, Chu S, Brunger AT. Single-molecule studies of synaptotagmin and complexin binding to the SNARE complex. Biophys J. 2005; 89:690–702. [PubMed: 15821166]
40. Rizo J, Rosenmund C. Synaptic vesicle fusion. Nat Struct Mol Biol. 2008; 15:665–674. [PubMed: 18618940]
41. Shao X, et al. Synaptotagmin-syntaxin interaction: the C2 domain as a Ca2+-dependent electrostatic switch. Neuron. 1997; 18:133–142. [PubMed: 9010211]
42. Giraudo CG, Eng WS, Melia TJ, Rothman JE. A clamping mechanism involved in SNARE-dependent exocytosis. Science. 2006; 313:676–680. [PubMed: 16794037]
43. Schaub JR, Lu X, Doneske B, Shin YK, McNew JA. Hemifusion arrest by complexin is relieved by Ca2+-synaptotagmin I. Nat Struct Mol Biol. 2006; 13:748–750. [PubMed: 16845390]
44. Huntwork S, Littleton JT. A complexin fusion clamp regulates spontaneous neurotransmitter release and synaptic growth. Nat Neurosci. 2007; 10:1235–1237. [PubMed: 17873870]
45. Zimmerberg J, Akimov SA, Frolov V. Synaptotagmin: fusogenic role for calcium sensor? Nat Struct Mol Biol. 2006; 13:301–303. [PubMed: 16715046]
46. Parsegian VA, Rand RP, Stamatoff J. Perturbation of membrane structure by uranyl acetate labeling. Biophys J. 1981; 33:475–477. [PubMed: 6164411]
47. Winiski AP, McLaughlin AC, McDaniel RV, Eisenberg M, McLaughlin S. An experimental test of the discreteness-of-charge effect in positive and negative lipid bilayers. Biochemistry. 1986; 25:8206–8214. [PubMed: 3814579]
48. Ubach J, Garcia J, Nittler MP, Sudhof TC, Rizo J. Structure of the Janus-faced C2B domain of rabphilin. Nat Cell Biol. 1999; 1:106–112. [PubMed: 10559882]
49. Deak F, et al. Rabphilin regulates SNARE-dependent re-priming of synaptic vesicles for fusion. EMBO J. 2006; 25:2856–2866. [PubMed: 16763567]
50. Xue M, et al. Distinct domains of complexin I differentially regulate neurotransmitter release. Nat Struct Mol Biol. 2007; 14:949–958. [PubMed: 17828276]
51. Lois C, Hong EJ, Pease S, Brown EJ, Baltimore D. Germline transmission and tissue-specific expression of transgenes delivered by lentiviral vectors. Science. 2002; 295:868–872. [PubMed: 11786607]

52. Chen X, et al. SNARE-Mediated Lipid Mixing Depends on the Physical State of the Vesicles. Biophys J. 2006; 90:2062–2074. [PubMed: 16361343]

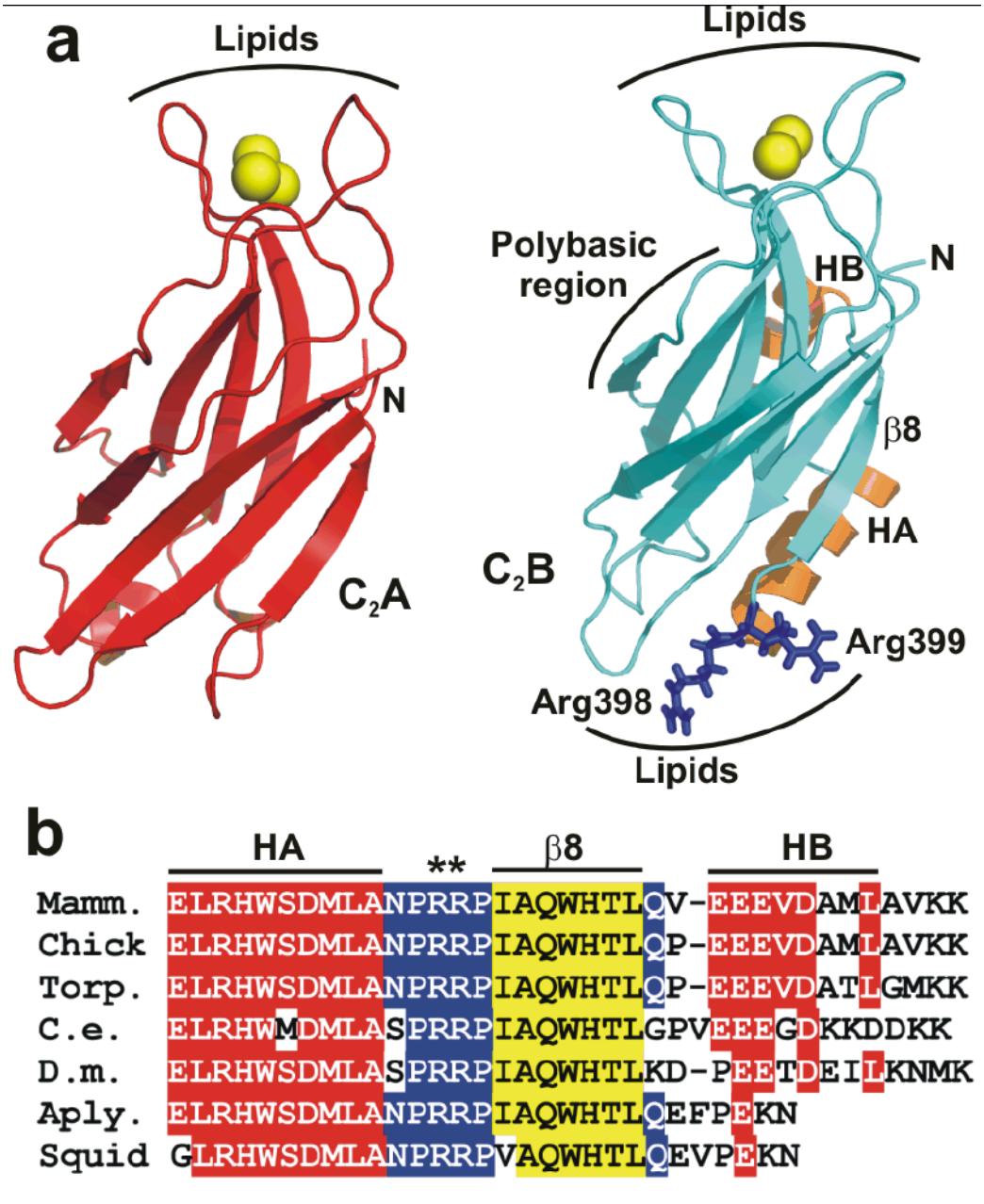

Figure 1.

Two highly conserved arginines at the bottom face of the synaptotagmin-1 C_2B domain. (**a**) Ribbon diagrams of the synaptotagmin-1 C_2A and C_2B domain7, 8 illustrating their structural differences. Ca^{2+} ions are shown as yellow spheres, helices HA and HB of the C_2B domain are colored in orange, and R398 and R399 are shown in blue stick models. Strand β8 of the C_2B domain is labeled. The lipid-binding sites of both C_2 domains are indicated. The binding site for the SNARE complex is tentatively assumed to be in the polybasic region on one side of the C_2B domain β-sandwich17, but note that this region has also been implicated in other interactions, including lipid binding25. (**b**) Sequence alignment

of the C-terminal region of synaptotagmin-1 C_2B domains from different species. Conserved residues are colored in red (helices HA and HB), blue (loops) and yellow (strand β8).

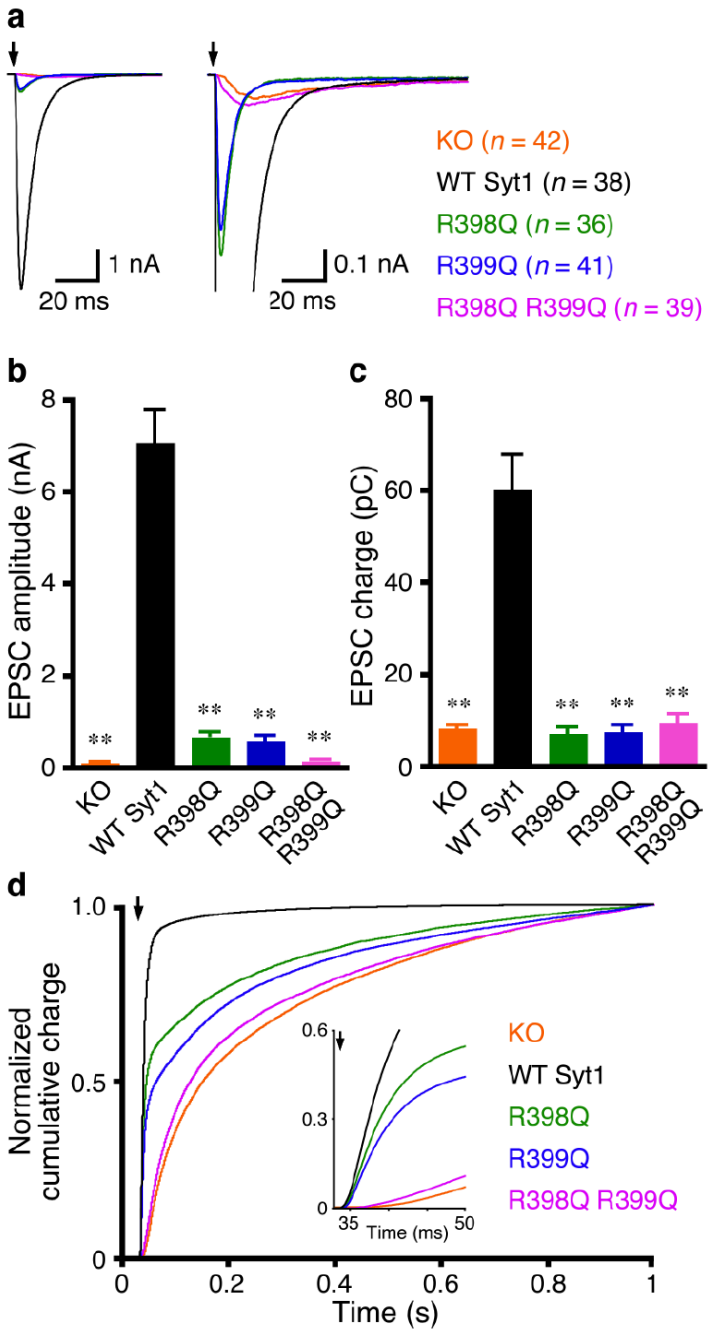

Figure 2.

The bottom face of the synaptotagmin-1 C_2B domain is critical for fast Ca^{2+}-triggered neurotransmitter release. (**a**) Average traces of basal evoked EPSCs of hippocampal synaptotagmin-1 KO neurons and KO neurons rescued with WT and mutant synaptotagmin-1 (Syt1) variants. Arrows represent 2–ms somatic depolarizations to 0 mV. Depolarization artifacts and action potentials were blanked. (**b**,**c**) Summary data of EPSC amplitude (**b**) and charge (**c**). Data are expressed as mean ± s.e.m. ** $P < 0.001$ as compared to KO neurons rescued by WT synaptotagmin-1. (**d**) Summary plot of the normalized

cumulative EPSC charge in 1 s. The inset shows the same normalized cumulative EPSC charge within the first 50 ms. Numbers of neurons analyzed in (**a-d**) are indicated in panel (**a**).

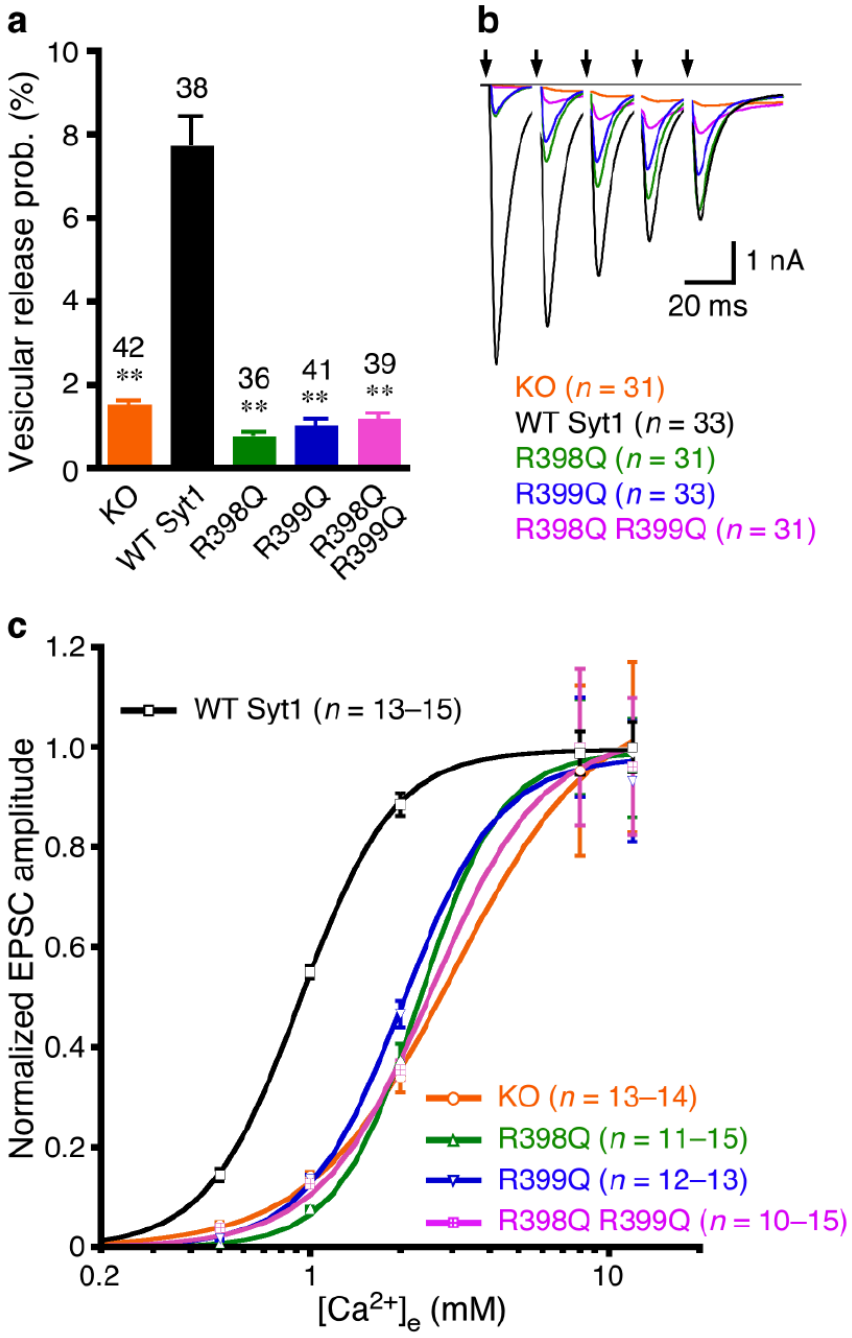

Figure 3.

The bottom face of the synaptotagmin-1 C_2B domain regulates probability and Ca^{2+}-sensitivity of release. (**a**) Summary data of vesicular release probability from synaptotagmin-1 KO neurons and KO neurons rescued with WT and mutant synaptotagmin-1 variants. Data are expressed as mean ± s.e.m. ** $P < 0.001$ as compared to KO neurons rescued by WT synaptotagmin-1. (**b**) Average traces of 5 consecutive EPSCs evoked at 50 Hz. Arrows represent 2–ms somatic depolarizations to 0 mV. Depolarization artifacts and action potentials were blanked. (**c**) Apparent Ca^{2+}-sensitivity of evoked release.

Normalized amplitudes of synaptic responses were plotted against external Ca^{2+} concentrations ($[Ca^{2+}]_e$). Data are expressed as mean ± s.e.m. and fitted with standard Hill equation. KO, K_d = 3.0 ± 0.2 mM, WT Syt1, K_d = 0.93 ± 0.01 mM, R398Q, K_d = 2.3 ± 0.1 mM, R399Q, K_d = 2.0 ± 0.1 mM, R398Q,R399Q, K_d = 2.6 ± 0.3 mM. Numbers of neurons analyzed in (**a**-**c**) are indicated in the panels.

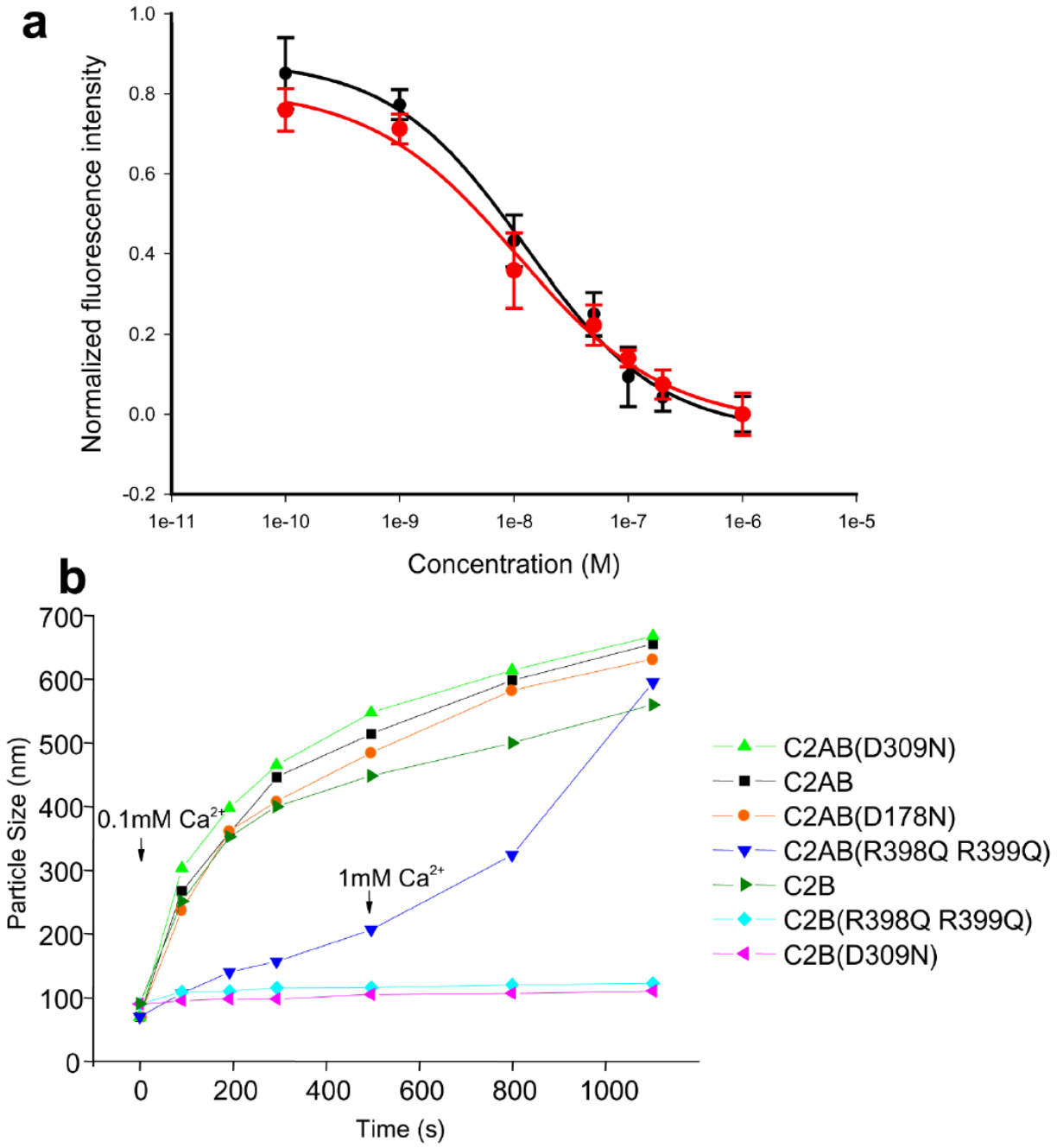

Figure 4.

The R398Q,R399Q mutation impairs synaptotagmin-1/membrane interactions. (**a**) The R398Q,R399Q mutation does not impair the ability of the C_2AB fragment to displace a complexin-1 fragment from membrane-anchored SNARE complexes. Supported phospholipid bilayers containing reconstituted SNARE complexes were deposited into microchannels, a rat complexin-1 fragment (residues 26-83) labeled with BODIPY-FL was bound to the SNARE complexes, and displacement of the labeled complexin 1 fragment by increasing concentrations of C_2AB fragment (black circles) or C_2AB-R398Q,R399Q

fragment (red circles) was monitored with a confocal fluorescence microscope as described17, 30. The data were normalized to the background fluorescence. Error bars represent SEMs derived from three separate measurements. Fitting of the data to a dose-response curved yielded an EC50 of 12 nM for both the WT and mutant C_2AB fragment, which is comparable to earlier results obtained for WT C_2AB fragment30. (**b**) The R398Q,R399Q mutation impairs the vesicle clustering activity of the C_2AB fragment. Mixtures of liposomes (100 nm average size) with WT or mutant C_2B domain or C_2AB fragment were prepared as described27, and the change in particle size as a function of time was measured by DLS after addition of 100 μM Ca^{2+}. For the experiment performed with the R398Q,R399Q mutant C_2AB fragment, 1 mM Ca^{2+} was added after 500 s.

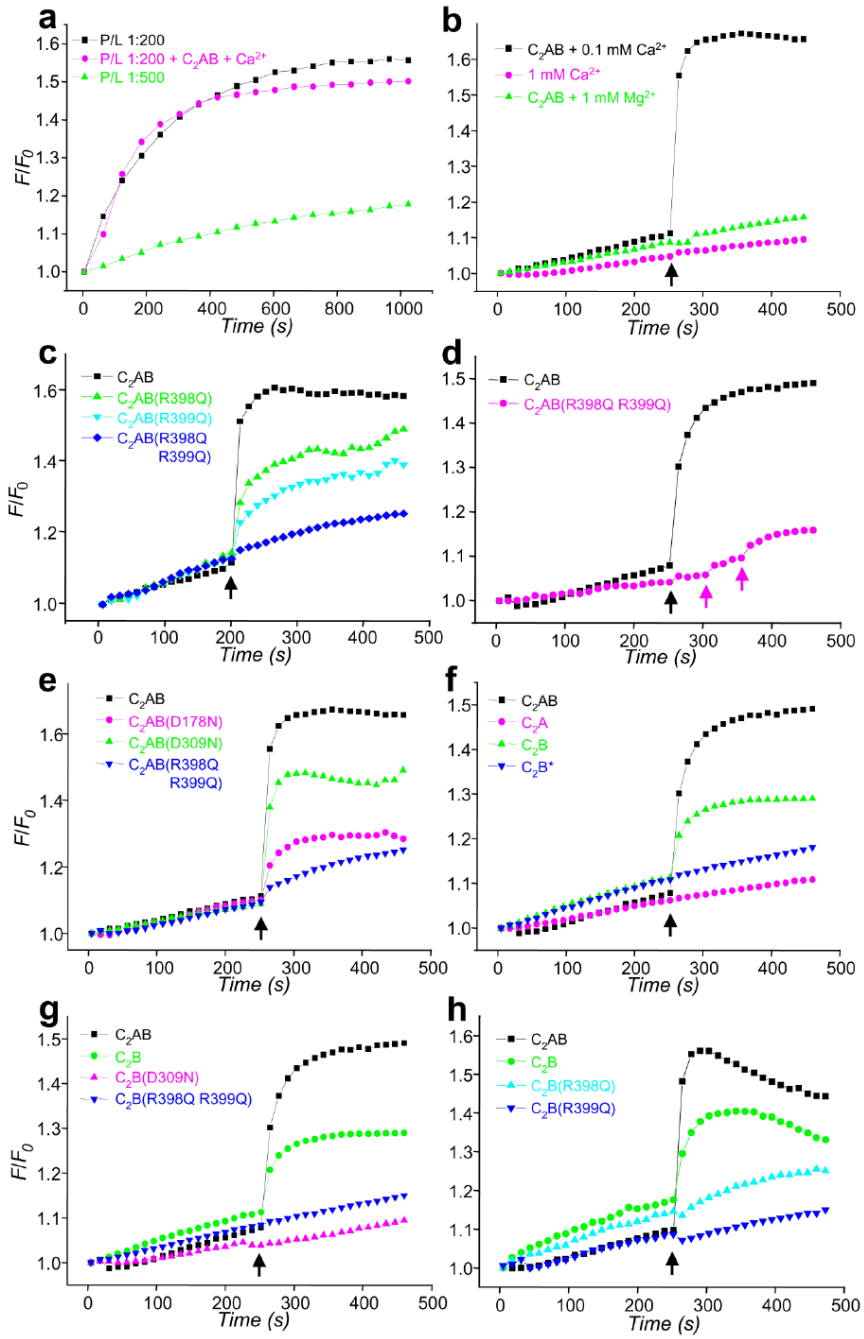

Figure 5.

Ca^{2+} and synaptotagmin-1 induce a drastic increase in the rate of SNARE-mediated lipid mixing that is abolished by the R398Q,R399Q mutation. (**a**) Lipid mixing between synaptobrevin- and syntaxin-1/SNAP-25-containing proteoliposomes with 1:200 (black) or 1:500 (green) P/L ratios. Equal amounts of the proteoliposomes were mixed, and lipid mixing was detected by monitoring lipid fluorescence dequenching. In all experiments, the syntaxin-1/SNAP-25 liposomes were preincubated with a C-terminal synaptobrevin fragment (residues 49-96). F/F_0 represents the fluorescence relative to the starting point. The

pink trace shows an experiment performed with a 1:200 P/L ratio in the presence of 1 μM C_2AB fragment and 100 μM Ca^{2+}. (**b-h**) Lipid-mixing assays were performed as in (**a**) with a 1:500 P/L ratio plus different additions as indicated. Synaptotagmin-1 fragments (1 μM) were added at the beginning of the fusion reaction. In (**b**), Ca^{2+} or Mg^{2+} was added after 250 s of reaction (black arrows) as indicated. In (**c-h**), 100 μM Ca^{2+} was added at 250 s (black arrows). In (**d**), subsequent additions of 200 μM and 1 mM Ca^{2+} for a reaction with the C_2AB-R398Q,R399Q mutant are indicated by pink arrows. WT and mutant C_2B domains were purified using our standard protocol36, except for one experiment where the WT C_2B domain was purified under less stringent conditions [indicated as C_2B*; blue triangles in (**f**)]. Each set of experiments shown in each panel was performed on the same day with the same proteoliposome preparations.

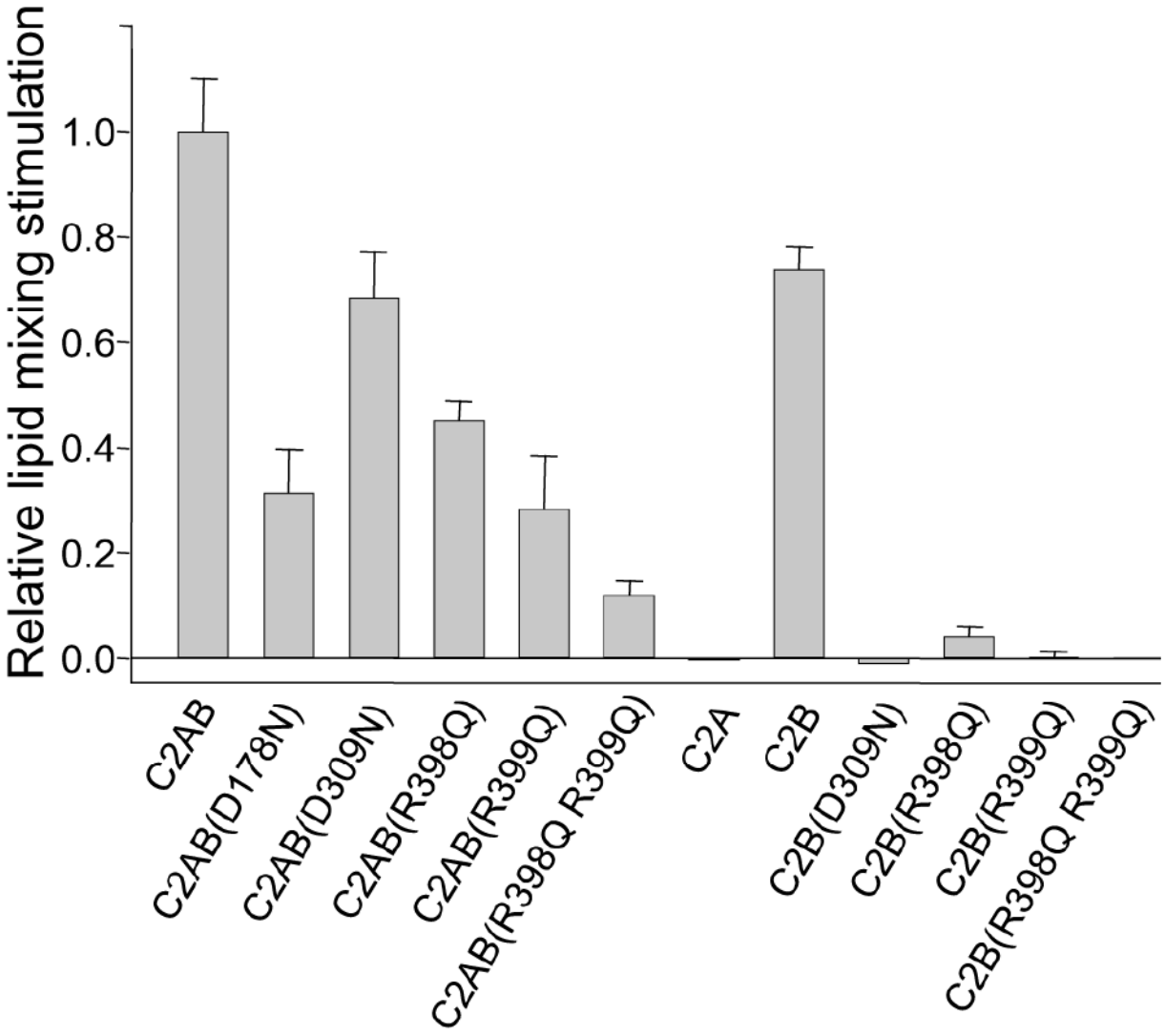

Figure 6.

Relative fusion stimulation activities of synaptotagmin-1 fragments. Lipid mixing assays analogous to those shown in Fig. 5 were performed for each synaptotagmin-1 fragment. The increase in F/F_0 during the 40 seconds following Ca^{2+} addition was measured, and the background Ca^{2+}-independent lipid mixing was subtracted by linear extrapolation from the data acquired before Ca^{2+} addition. The resulting values were normalized to the average F/F_0 increase observed for the WT C_2AB fragment in parallel experiments with the same proteoliposome concentrations. Error bars show standard deviations from triplicate experiments.

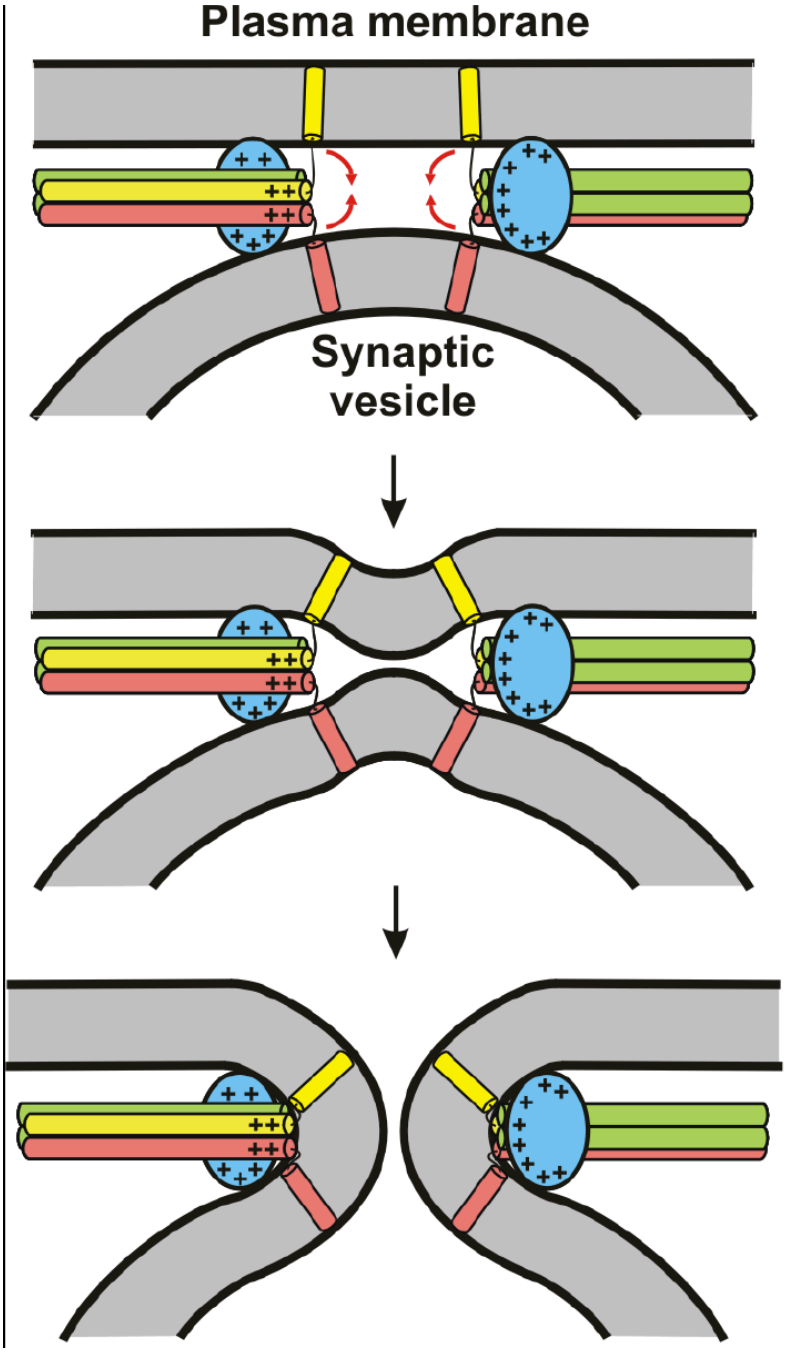

Figure 7.

Proposed mode of how the synaptotagmin-1 C_2B domain and the SNARE complex cooperate in Ca^{2+}-triggered membrane fusion. The C_2B domain is colored in blue, syntaxin in yellow, SNAP-25 in green and synaptobrevin in pink. The C_2A domain (not shown for simplicity) is predicted to help in release by binding to one of the membranes, but could have additional roles that remain to be demonstrated. The model predicts that the Ca^{2+}-binding loops at the top of the C_2B domain bind to one membrane, the bottom face to the other membrane, and the polybasic region to the SNARE complex (see Fig. 1a for the

locations of these structural elements in the C_2B domain structure). In principle, the Ca^{2+}-binding loops could act either on the vesicle or the plasma membrane. The + signs illustrate the abundance of positive charges in the C_2B domain and the C-terminus of the SNARE complex [see ref. 17]. The red arrows in the top diagram indicate that these positive charges likely help to attract the lipids toward the center, inducing negative curvature on the membranes to initiate fusion.